



Published in final edited form as:

Opt Express. 2008 October 27; 16(22): 18551–18556.

Realtime Photoacoustic Microscopy of Murine Cardiovascular Dynamics

R.J. Zemp^{1,3,*}, L. Song^{1,*}, R. Bitton², K.K. Shung², and L.V. Wang^{1,*}

¹Washington University, Optical Imaging Laboratory, Department of Biomedical Engineering, St. Louis, MO 63130

²University of Southern California, Department of Biomedical Engineering, Los Angeles, CA 90089

³University of Alberta, Department of Electrical & Computer Engineering, Edmonton, Alberta, Canada, T6G 2V4

Abstract

Non-invasive visualization of cardiovascular dynamics in small animals is challenging due to their rapid heart-rates. We present a realtime photoacoustic imaging system consisting of a 30-MHz ultrasound array transducer, receive electronics, a high-repetition-rate laser, and a multicore-computer, and demonstrate its ability to image optically-absorbing structures of the beating hearts of young athymic nude mice at rates of ~50 frames per second with $100\ \mu\text{m} \times 25\ \mu\text{m}$ spatial resolution. To our knowledge this is the first report of realtime photoacoustic imaging of physiological dynamics.

1. Introduction

Due to the rapid heart rates of mice, cardiovascular research utilizing murine models of disease requires high frame-rate imaging modalities. Presently, widely used small animal imaging techniques such as micro-PET and micro-CT do not permit imaging frame rates sufficient for murine cardiovascular visualization. High-frequency ultrasound has emerged as a valuable tool for cardiovascular research, offering both high resolution and high frame rates [1]. Beyond tissue structure and morphology, imaging systems offering functional imaging capabilities are highly desirable for cardiovascular research. Of particular interest is measurement of blood flow, which high-frequency ultrasound can provide, and estimation of local blood or tissue oxygenation, which ultrasound alone cannot. However, an emerging bio-imaging technology, photoacoustic imaging, has the potential for noninvasive oxygenation mapping [2]. This letter describes a unique realtime photoacoustic imaging system and its application in imaging the beating hearts of young athymic nude mice in vivo.

Photoacoustic imaging uses laser-induced ultrasound to form images of optical pigmentation in subcutaneous tissue [3]. Photoacoustic signal strength is proportional to the local optical absorption coefficient of tissue, and scales in magnitude with the optical fluence delivered. Dominant subcutaneous absorbing pigments include oxy-hemoglobin and deoxy-hemoglobin, hence high contrast images of blood vessels and microvessels are possible [4]. With multiple optical wavelengths sequentially used to interrogate tissue, algorithms akin to those used in

© 2007 Optical Society of America

*Equal contribution zemp@ece.ualberta.ca

*Corresponding author: lhwang@biomed.wustl.edu

OCIS codes: (110.5120) Photoacoustic imaging; (110.5100) Phased-array imaging systems; (110.7170) Ultrasound; (170.3880) Medical and biological imaging; (170.3890) Medical optics instrumentation.

pulse-oximeters may be used to estimate blood oxygen saturation [5]. Additionally, photoacoustic technologies have been shown to be promising for molecular imaging, including gene expression imaging [6].

Recently, our group demonstrated a novel realtime photoacoustic imaging system based on a high-repetition-rate laser and a high-frequency ultrasound array transducer [7,8]. In this letter, we report on the refinement of this system and its use for imaging in realtime the beating hearts of mice. To our knowledge, along with our recent conference paper, this is the first published report of realtime photoacoustic imaging of physiological dynamics.

2. Methods

Our system design is described in detail in [8], however we report the most salient features here, highlighting our current experimental protocol. An Nd:YLF Q-switched laser delivering 523-nm light pulses of 6-8-ns duration at up to 12 mJ of pulse energy, and up to 1 KHz repetition rates was used to pump a tunable dye laser circulating Rhodamine 6G laser dye. The tunable laser output was fiber-coupled into a 600- μm high-numerical aperture optical fiber, and the light at the other end of the fiber was directed obliquely onto the imaging subject, forming an elliptical illumination pattern with $\sim 10 \text{ mJ/cm}^2$ incident laser fluence. A custom high-frequency ultrasound array transducer (fabricated in the NIH Transducer Resource Group, [9]), was used to receive high-frequency photoacoustic signals. The array possessed 48 elements with 30-MHz center frequency, $2\text{-}\lambda$ pitch, and 8.2 mm elevational focus. Custom receive and control electronics were used to amplify and multiplex received acquisitions, and an 8-channel PCI digitizer with 125 MS/s parallel digitization rate was used to acquire, digitize, and stream received photoacoustic signal data to the RAM of a dual-socket quad-core PC (possessing 8 processor cores). Realtime delay-and-sum beamforming was implemented using parallel programming on these processor cores, while scan conversion was offloaded to the Graphical Processing Unit of the video card. The PCI digitizer served as master clock, and generated 6 trigger-out signals at 1 KHz repetition rate to the laser to acquire 48-channels of data using 6 multiplexed acquisitions. One multiplexed acquisition of the 48-channels was then used to form a single B-scan image frame, and inter-frame triggering was software generated, averaging ~ 50 frames per second. The system resolution was quantified as $\sim 100 \mu\text{M}$ laterally, and $25 \mu\text{M}$ axially.

In this paper the laser trigger-signal from the PCI digitizer was also routed through a pulse-delay generator to an oscilloscope. Simultaneously another channel of the oscilloscope was used to record pulse-oximeter signals. The pulse-delay generator output a TTL pulse 7 ms in duration for the first trigger pulse it encountered, so that the train of 6 trigger pulses was effectively converted to a single TTL pulse for each image frame. The oscilloscope was hence used to record the occurrence of image frames relative to the cardiac cycle to validate that we were indeed imaging the heart in realtime, and not temporally under-sampling.

Young athymic nude mice (10 g) were purchased from Charles River Laboratories. Nude mice were anesthetized using a gas anesthesia machine according to approved protocols, and maintained under anesthesia using this machine throughout the imaging procedure. A pulse-oximeter probe was clamped to a hind-paw, and the animal was positioned so that its chest wall was facing the ultrasound transducer. The mouse was laid on a lab-jack with a soft plastic insulating bed. Fore- and hind-paws were secured to the lab-jack with adhesive tape. A thin layer of acoustic coupling gel was applied to the mouse, then the lab-jack and animal were raised up to an optically-and acoustically transparent water-filled membrane (Saran Premium WrapTM, SC Johnson Inc.) sagging from an aperture in a water tank. The purpose of this water tank was to serve as an acoustic coupling mechanism for photoacoustic signals, and as an optically transparent medium for light delivery. The photoacoustic probe, consisting of the

optical fiber and ultrasound array transducer were lowered into the water tank, and positioned with the aid of a 3-axis translation stage. Realtime display from our imaging system was also invaluable for probe positioning. Following animal positioning, computer-console control of the imaging system was used to initiate data recording. In deep anesthesia, animal heart rates recorded by the pulse-oximeter and oscilloscope averaged 180-240 beats per minute or 3-4 beats per second. The realtime imaging speed with realtime data archival to the hard-drive could be performed at rates as high as 50 frames per second, adequate for capturing several image frames per cardiac cycle.

3. Results

Fig. 2 shows a video of the imaging system and realtime display, demonstrating visualization of the beating heart. Fig. 3 shows a movie of the beating heart of the same mouse, while rendered offline. Fig. 4 shows an M-mode image, consisting of A-scan lines from the midpoint of Fig. 3 as a sequence of time. The motion of an absorbing structure is apparent as a periodic motion. Two gaps in the cardiac cycle are evident and attributed to respiratory-induced motion. Structures are visualized to depths of ~3-4 mm, roughly 1/3 of the estimated body thickness during the imaging procedure. The B-scan photoacoustic images shown here offer visualization of optically absorbing structures, and their motion with cardiac and respiratory cycles is evident. The images shown here were acquired with a single optical wavelength of 578-nm, an isosbestic point (i.e. a point where deoxy- and oxy-hemoglobin molar extinction coefficient are equal). With this wavelength, oxygenated blood is visualized with the same contrast as deoxygenated blood.

4. Discussion

Presently, delineation of cardiac structures is difficult, however, complementary co-registered high-frequency ultrasound may serve this role in future work. Nevertheless, our system offers optical absorption contrast rather than ultrasound backscatter contrast, and these preliminary image sequences are the first of their kind. Image quality is expected to improve with future system improvements.

Active adult mice may have heart-rates from 400 to as high as 800 beats per minute (bpm) which may challenge our present 50 fps system. However, it is known that very young mice such as those used in our study, have lower heart-rates (286 \pm 56 bpm for newborns [10]). Additionally, anesthetized mice may have lower heart-rates (anesthetic-dependent rates as low as 200 beats per minute for adult mice are reported in [11]). Hence the observed heart-rates are roughly consistent with the literature. In other data not shown we are able to image 300 bpm heart-rates. Deep breaths apparent in the movie and the M-mode data may suggest that improvements in animal positioning techniques are warranted.

Of considerable interest is the noticeable change in visibility of vessels during respiration, and may be due to venule expansion during respiratory-induced intra-thoracic pressure changes. This effect is worthy of further future study, and may prove important for studying venous return and diastolic function. These observations also motivate photoacoustic technology as a candidate for functional imaging studies, where a stimulus induces local vasoconstriction or vasodilation. Future work should also use multiple wavelengths for blood oxygenation estimation. This capability will prove important for studying ischemia in cardiovascular disease. Distinct from perfusion, oxygen saturation of tissues will provide important information linking tissue behavior to oxidative stress. Oxygen saturation may also be important for studying developmental causes, consequences, and solutions to septal defects where oxygenated and deoxygenated blood mix during cardiac cycles. With future improvements, photoacoustic imaging technology may also help us understand hemodynamics

in small animals with information which ultrasound alone cannot provide. Beyond small animal cardiovascular research, realtime photoacoustic imaging may serve an important future role in clinical settings, and we anticipate a bright future for this emerging technology.

Acknowledgements

We thank the NIH transducer resource group for their work in fabrication of the high-frequency ultrasound transducer. This work was supported by NIH grants R01 EB000712 and R01 NS46214.

References and Links

1. Foster FS, Zhang MY, Zhou YQ, Liu G, Mehi J, Cherin E, Harasiewicz KA, Starkoski BG, Zan L, Knapik DA, Adamson SL. A new ultrasound instrument for in vivo microimaging of mice. *Ultrasound in Medicine and Biology* 2002;28:1165–1172. [PubMed: 12401387]
2. Zhang HF, Maslov K, Stoica G, Wang LHV. Functional photoacoustic microscopy for high-resolution and noninvasive in vivo imaging. *Nature Biotechnology* 2006;24:848–851.
3. Xu MH, Wang LHV. Photoacoustic imaging in biomedicine. *Review of Scientific Instruments* 2006;77
4. Zhang E, Beard P. Broadband ultrasound field mapping system using a wavelength tuned, optically scanned focused laser beam to address a Fabry Perot polymer film sensor. *Ieee Transactions on Ultrasonics Ferroelectrics and Frequency Control* 2006;53:1330–1338.
5. Sivaramakrishnan M, Maslov K, Zhang HF, Stoica G, Wang LV. Limitations of quantitative photoacoustic measurements of blood oxygenation in small vessels. *Physics in Medicine and Biology* 2007;52:1349–1361. [PubMed: 17301459]
6. Li L, Zemp RJ, Lungu G, Stoica G, Wang LHV. Photoacoustic imaging of lacZ gene expression in vivo. *Journal of Biomedical Optics* 2007;12:020504 1–3. [PubMed: 17477703]
7. Zemp RJ, Bitton R, Li ML, Shung KK, Stoica G, Wang LV. Photoacoustic imaging of the microvasculature with a high-frequency ultrasound array transducer. *J Biomed Opt* 2007;12:010501. [PubMed: 17343475]
8. Zemp R, Song L, Bitton R, Shung K, Wang L. Realtime photoacoustic microscopy in vivo with a 30-MHz ultrasound array transducer. *Optics Express* 2008;16:7915–7928. [PubMed: 18545502]
9. Cannata JM, Williams JA, Zhou QF, Ritter TA, Shung KK. Development of a 35-MHz piezo-composite ultrasound array for medical imaging. *Ieee Transactions on Ultrasonics Ferroelectrics and Frequency Control* 2006;53:224–236.
10. Richards AG, Simonson E, Visscher MB. Electrocardiogram and Phonogram of Adult and Newborn Mice in Normal Conditions and Under the Effect of Cooling, Hypoxia and Potassium. *Am J Physiol* 1953;174:293–298. [PubMed: 13080449]
11. Kramer K, E. Vanacker SAB, Voss HP, Grimbergen JA, Vandervijgh WJF, Bast A. Use of Telemetry to Record Electrocardiogram and Heart-Rate in Freely Moving Mice. *Journal of Pharmacological and Toxicological Methods* 1993;30:209–215. [PubMed: 8123902]

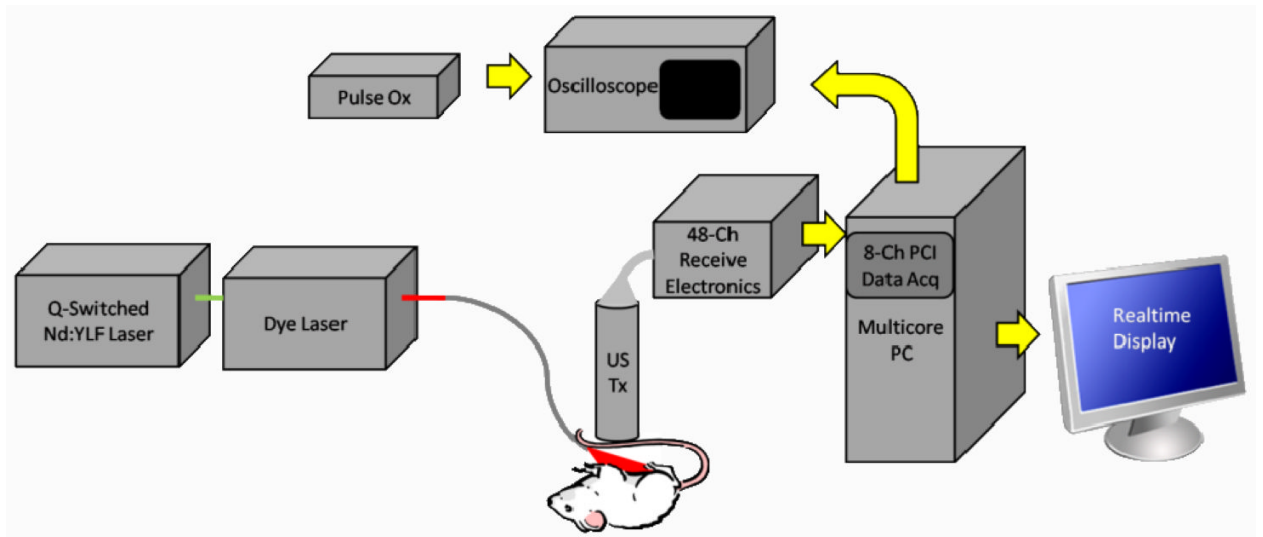


Figure 1.

Diagram of our photoacoustic imaging system. A tunable pulsed laser system delivers light via an optical fiber to the animal subject. A high frequency ultrasound array transducer (US Tx) receives the photoacoustic signals, which are amplified and de-multiplexed using custom receive electronics, then digitized using an 8-channel PCI data acquisition card. A computer with 8 processor cores performs realtime beamforming and display. A pulse oximeter (Pulse Ox) was used to monitor animal health and measure animal heart rates.

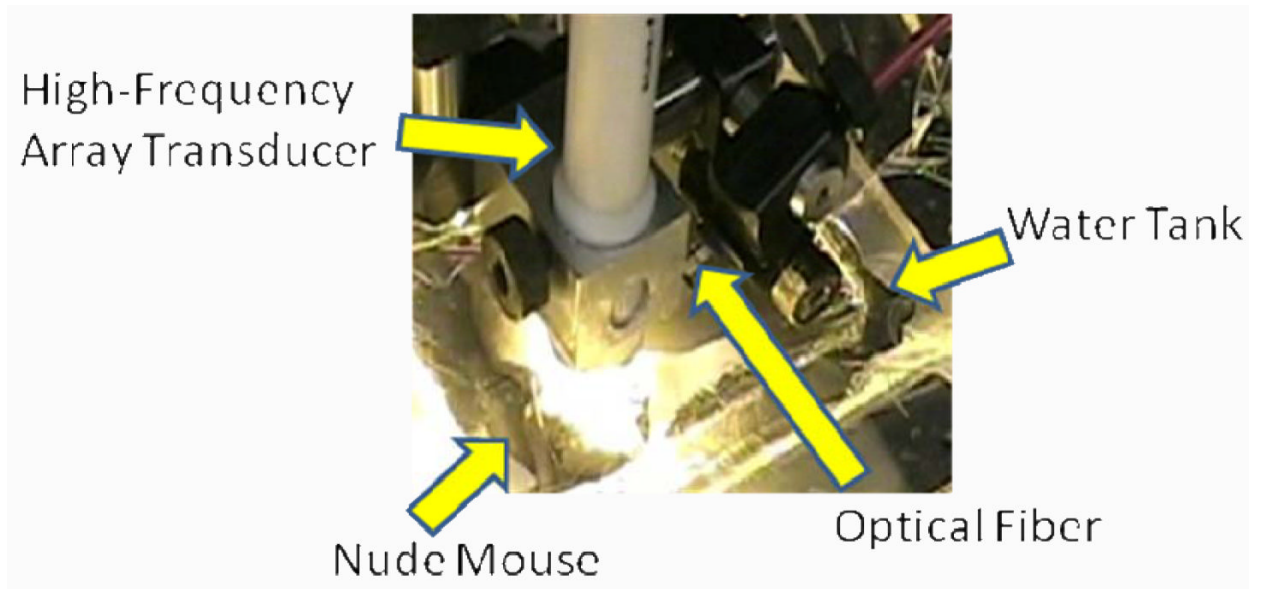


Figure 2.
(1.8MB) Video of the realtime photoacoustic imaging system and realtime display while imaging the beating heart of an athymic nude mouse.

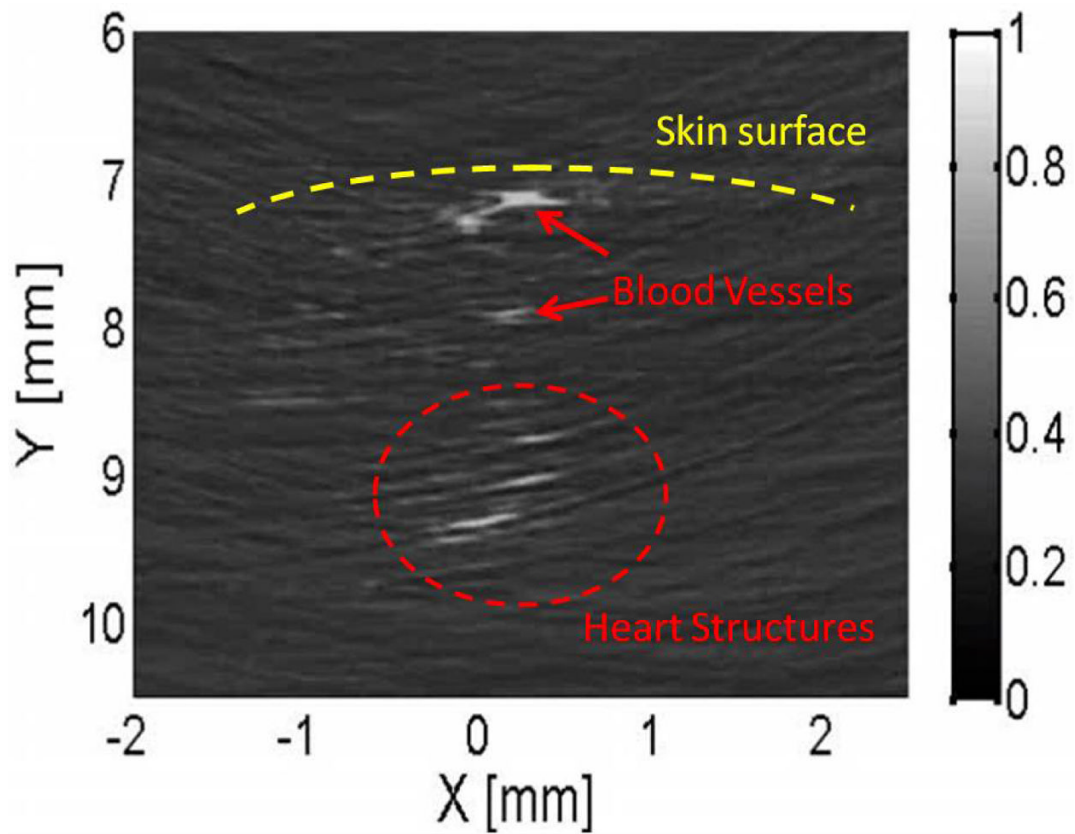


Figure 3.
(3 MB) Photoacoustic B-scan movie of the beating heart of an athymic nude mouse. This movie sequence was reconstructed and rendered offline using data archived in realtime.

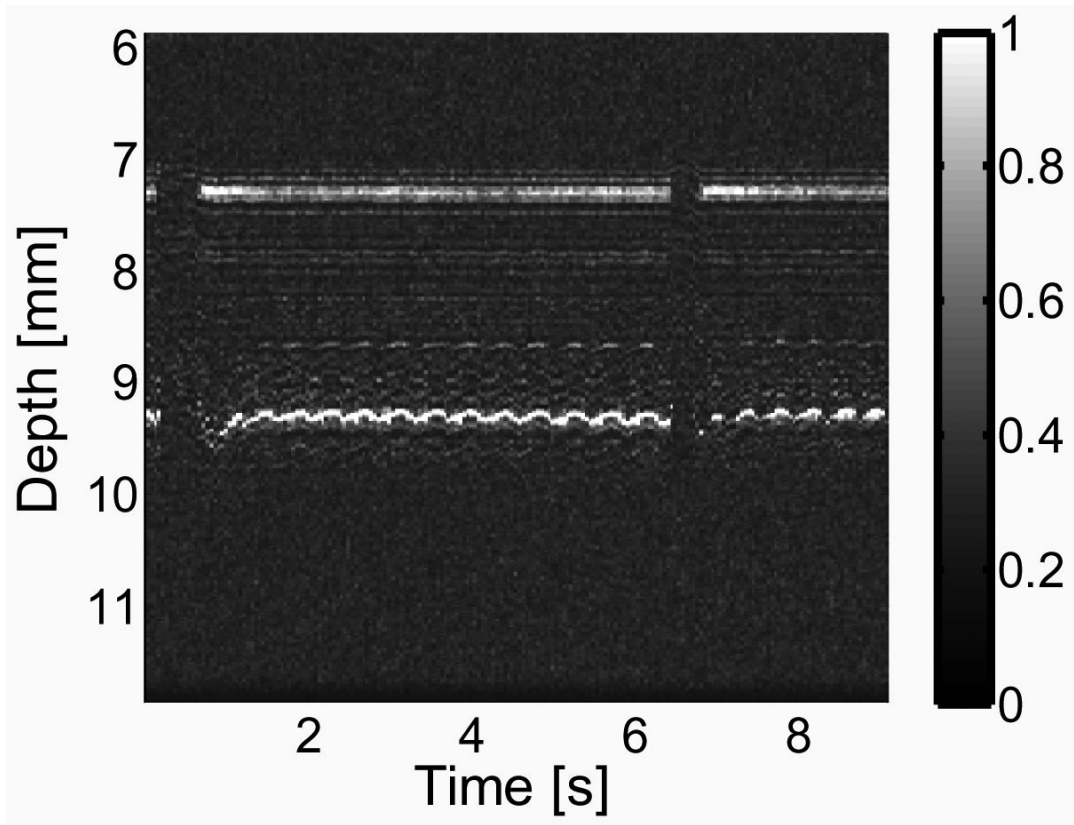


Figure 4.

M-mode image along the X=0 mm line in Fig. 3. The oscillating structures around the 9-mm depth below the transducer surface show the cardiac motion as a function of time. The animal's heart estimated here as ~ 3 beats per second corresponded well to the 180 beats per minute as measured by the pulse oximeter.